AD NUMBER

AD435861

NEW LIMITATION CHANGE

TO

Approved for public release, distribution unlimited

FROM

Distribution authorized to U.S. Gov't. agencies and their contractors; Adminstrative and Operational Use; Apr 1964. Other requests shall be referred to the Air Force Arnold Engineering Development Center, Attn: STINFO, Arnold AFB, TN 37389.

AUTHORITY

AFFDL ltr 21 Oct 1974

AEDC-TDR-64-65

PRESSURE MEASUREMENTS ON THE RIGID MODEL OF A BALLOON DECELERATOR IN THE WAKE OF A SIMULATED MISSILE PAYLOAD AT MACH NUMBERS 1.5 TO 6.0

By

D. R. Bell
von Kármán Gas Dynamics Facility
ARO, Inc.

TECHNICAL DOCUMENTARY REPORT NO. AEDC-TDR-64-65

April 1964

Program Element 620405334/8151

(Prepared under Contract No. AF 40(600)-1000 by ARO, Inc., contract operator of AEDC, Arnold Air Force Station, Tenn.)

ARNOLD ENGINEERING DEVELOPMENT CENTER

AIR FORCE SYSTEMS COMMAND

UNITED STATES AIR FORCE

NOTICES

AEDC-TDR-64-65

PRESSURE MEASUREMENTS ON THE RIGID MODEL OF A BALLOON DECELERATOR IN THE WAKE OF A SIMULATED MISSILE PAYLOAD AT MACH NUMBERS 1.5 TO 6.0

By

D. R. Bell
von Kármán Gas Dynamics Facility
ARO, Inc.
a subsidiary of Sverdrup and Parcel, Inc.

April 1964

ARO Project No. VA0404

ABSTRACT

Tests were made on a rigid model of a balloon decelerator (Ballute) positioned at various axial locations in the wake of a cone-cylinder flare model. Pressure data were obtained on the Ballute model, and pressure surveys were made in the wake of the cone-cylinder flare model. The tests were made in Tunnel A of the von Kármán Gas Dynamics Facility at Mach numbers from 1.5 to 6 and at Reynolds numbers, based on the parent body length, from 1.42 to 2.35 x 10^6. Pressure distribution data on the Ballute model and pitot pressure survey data in the wake are presented.

PUBLICATION REVIEW

This report has been reviewed and publication is approved.

Darreld K. Calkins
Major, USAF
AF Representative, VKF
DCS/Test

Jean A. Jack
Colonel, USAF
DCS/Test

CONTENTS

TABLE

ILLUSTRATIONS

NOMENCLATURE

d	Base diameter of missile, 2 in.
d'	Maximum diameter of decelerator excluding burble fence, 7.5 in.
ℓ	Axial distance aft of theoretical nose of decelerator, in.
M_∞	Free-stream Mach number
p_n	Static pressure on decelerator surface, psia
p_o	Free-stream total pressure, psia
p_w'	Pitot pressure measured by wake survey rake probes, psia
p_∞	Free-stream static pressure, psia
Re	Reynolds number, based on parent model length of 14.23 in.
r	Radial distance from decelerator centerline, in.
T_o	Free-stream total temperature, °R
x	Axial distance from base of missile to decelerator, in. (see Fig. 2)

1.0 INTRODUCTION

Tests were conducted on a rigid model of a balloon decelerator (Ballute) positioned at various longitudinal stations in the wake of a cone-cylinder flare model simulating a missile payload. The tests were conducted on January 3 and 6, 1964, in the 40-in. supersonic tunnel (Gas Dynamic Wind Tunnel, Supersonic (A)) of the von Kármán Gas Dynamics Facility (VKF), Arnold Engineering Development Center (AEDC), Air Force Systems Command (AFSC), for the Goodyear Aircraft Corporation, Akron, Ohio, and were sponsored by the Air Force Flight Dynamics Laboratory (AFFDL), AFSC.

Pressure measurements on the decelerator and in the wake of the parent body just ahead of the decelerator were made at Mach numbers from 1.5 to 5 in half Mach number increments and at Mach number 6. The Reynolds number, based on the parent body length, varied from 1.38×10^6 at Mach 1.5 and 0.9×10^6 at Mach 2 up to 2.35×10^6 at Mach 6.

This test was part of a study by the Goodyear Aircraft Corporation to determine the feasibility of inflatable balloon-type drag devices for applications such as first-stage deceleration of emergency escape capsules, booster assemblies, and missile components.

2.0 APPARATUS

2.1 WIND TUNNEL

Tunnel A (Fig. 1) is a continuous, closed circuit, variable density wind tunnel with an automatically driven, flexible plate-type nozzle. The tunnel operates at Mach numbers from 1.5 to 6 at maximum stagnation pressures from 29 to 200 psia, respectively, and stagnation temperatures up to 300°F ($M_\infty = 6$). Minimum operating pressures are about one-tenth of the maximum at each Mach number. A complete description of the tunnel and airflow calibration information is given in Refs. 1 and 2.

2.2 MODEL

A 7.5-in.-diam rigid decelerator model (wood construction) and a 2-in.-diam missile model (aluminum) were supplied by the Goodyear

---

Manuscript received March 1964.

Aircraft Corporation for this test. A sketch of the models is shown in Fig. 2 and an installation photograph in Fig. 3. The decelerator model was sting mounted on the tunnel sector in a fixed position, and the missile was attached to the decelerator by a telescoping actuator which provided variation of the separation distance between the missile and decelerator models. This actuator was manually extended or collapsed by a push-pull mechanism consisting of a piano wire attached to the forward end of the actuator and running aft, through the decelerator, out of the tunnel. Several dummy inlets of varying geometry were built into the surface of the decelerator to help determine the optimum location and configuration for the inflating inlets.

The decelerator was instrumented with two rays of static pressure orifices, inlet pressure orifices, a pitot rake, and a wake survey rake. The wake rake consisted of 8 pitot pressure probes and 2 static pressure probes. General arrangement of the pressure orifices is shown in Fig. 2; the orifice locations are included in the figures of the pressure results. The primary function of the missile model was to create a wake for the decelerator; hence, this model was not instrumented.

2.3 INSTRUMENTATION AND PRECISION OF MEASUREMENTS

All model pressures were measured with the Tunnel A pressure scanning system utilizing 1- and 15-psid transducers referenced to a near vacuum. Each transducer was calibrated for three pressure ranges to give full-scale readings of 0.16, 0.40, and 1.0 psia for the 1-psid transducers and 2.4, 6, and 15 psia for the 15-psid transducers. The precision of measurement for the system is considered to be within 1 percent of full scale for each calibrated range. The tunnel stagnation pressure was measured with 15-, 30-, 60-, or 150-psid pressure transducers which were referenced to a near vacuum. These transducers are considered to have a precision of measurement of 0.1-percent full scale. The Mach number distribution within a 12-in. radius of the Tunnel A centerline is uniform to within about ±0.5 percent.

3.0 RESULTS AND DISCUSSION

Data were taken with the missile removed and with the missile at x/d values (separation distance to missile base diameter) of 6.00, 7.12, 9.00, 11.00, and 12.00 for each one-half Mach number increment from Mach 1.5 to 5 and at Mach 6.

Figures 4 through 8 present selected results showing decelerator surface pressure distributions, missile wake pitot pressure distribution, and schlieren photographs at Mach numbers 2, 3, 4, and 5. In general, data are presented for the maximum and minimum separation distances and with the missile removed. Data for intermediate separation distances are presented only where significant changes in the decelerator flow field occurred. Pressure distributions are presented for only one of the surface static pressure rays since both rays showed essentially the same variation.

Figure 4 shows that the decelerator pressure distributions are similar throughout the range of separation distance tested, and the schlieren photographs of this figure show that the missile wake is convergent throughout this range. The decelerator pressures reflect the low energy flow of the missile wake by a surface pressure deficit over the forward portion of the decelerator and a decrease in the pitot pressures of the wake survey rake as the decelerator centerline is approached. This pressure distribution is typical for the convergent missile wake, although, in this instance, the surface pressure decrease on the missile nose and the nonuniformity of the pitot pressure is apparently accentuated by the shock wave standing just ahead of, and impinging on, the survey rake. The effect of this shock wave can be seen more clearly at Mach 4 (Fig. 6).

Figure 5 shows that the decelerator flow field at Mach 3 remains, as at Mach 2, relatively unchanged throughout the range of separation distance tested, and the schlieren photographs indicate a convergent wake. The pressure distributions show the same general characteristics seen at Mach 2; however, the pitot pressure profiles are considerably more uniform than at Mach 2 because the shock wave just ahead of the decelerator is aft of the wake probe.

The decelerator flow field at Mach 4 is shown by Fig. 6 to be more varied than at Mach numbers 2 and 3. At the minimum separation distance ($x/d = 6.00$), the schlieren photograph shows a divergent missile wake. Both the surface static and wake pitot pressure distributions reflect this condition by a large pressure decrease when compared to the convergent wake ($x/d = 7.12$) and decelerator alone conditions. At $x/d = 9.00$, a strong shock wave is standing in front of the decelerator and impinges upon the wake pitot probe rake; the pressure distributions reflect this condition by the decreased pressures discussed earlier with regard to the Mach 2 data. It is interesting to note that this shock wave appears only at $x/d = 9.00$ and not at the closer separation distance $x/d = 7.12$.

Figure 7 shows that the divergent wake conditions seen at Mach 4 are not present at Mach 5. The closed wake, which is shown by the schlieren photographs at the maximum and minimum separation distances, occurred at all missile positions tested. This congruity of the flow conditions is also reflected in the similarity of the pressure distributions at the maximum and minimum x/d values.

Figure 8 shows that at Mach 6 the separation distance had a definite effect on the decelerator flow field. At x/d values between 6.00 and 9.00, both the schlieren photographs and the pressure distribution show that the missile wake is divergent, while at x/d = 11.00 and 12.00, the wake is convergent. The schlieren photograph for x/d = 6 also shows that the flow is separated over most of the missile at this condition.

4.0 CONCLUSIONS

The following results were obtained from tests of a rigid model of a balloon decelerator in the wake of a flared cone cylinder.

1. The decelerator pressures reflect the low energy flow of the missile wake by a pressure deficit when the data taken in the presence of the missile are compared to data taken with the decelerator alone.
2. For this particular system of missile, decelerator, and free-stream flow conditions, the missile wake remained convergent for all separation distances tested (x/d = 6.00 to 12.00) at Mach numbers 2, 3, and 5. At Mach 4 the missile wake diverged at x/d = 6.00 but converged at the larger separation distances. At Mach 6 the wake diverged at separation distances of x/d = 9.00 or less.

REFERENCES

1. Test Facilities Handbook (5th Edition). "von Kármán Gas Dynamics Facility, Vol. 4." Arnold Engineering Development Center, July 1963.
2. Coats, J. D. "Flow Characteristics of a 40-inch Wind Tunnel at Mach Numbers 1.5 to 6.0." AEDC-TDR-62-130, June 1962.

TABLE 1

RUN SUMMARY

M_∞	x/d					Decelerator Alone	p_o, psia	T_o, °R	Re x 10^{-6}
	6.00	7.12	9.00	11.00	12.00				
1.5	x	x	-	-	-	x	3.5	508	1.38
2.0	x	x	x	x	x	x	2.8	512	0.91
2.5	x	x	x	x	x	x	3.9	508	1.05
3.0	x	x	x	x	x	x	6.0	508	1.24
3.5	x	x	x	x	x	-	9.1	508	1.42
4.0	x	x	x	x	x	x	13.9	514	1.64
4.5	x	x	x	x	x	x	20.9	545	1.76
5.0	x	x	x	x	x	x	30.2	579	1.82
6.0	x	x	x	x	x	x	62.7	613	2.35

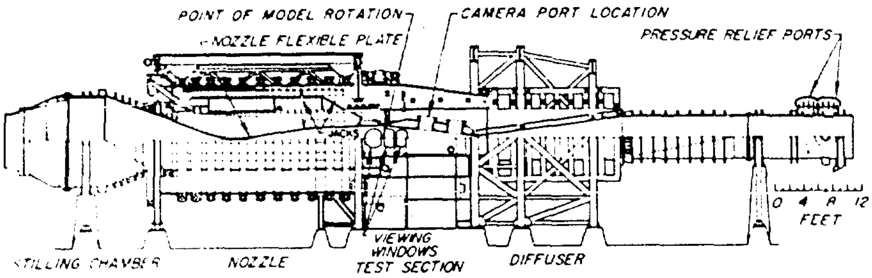

a. Tunnel Assembly

b. Nozzle and Test Section

Fig. 1 Tunnel A

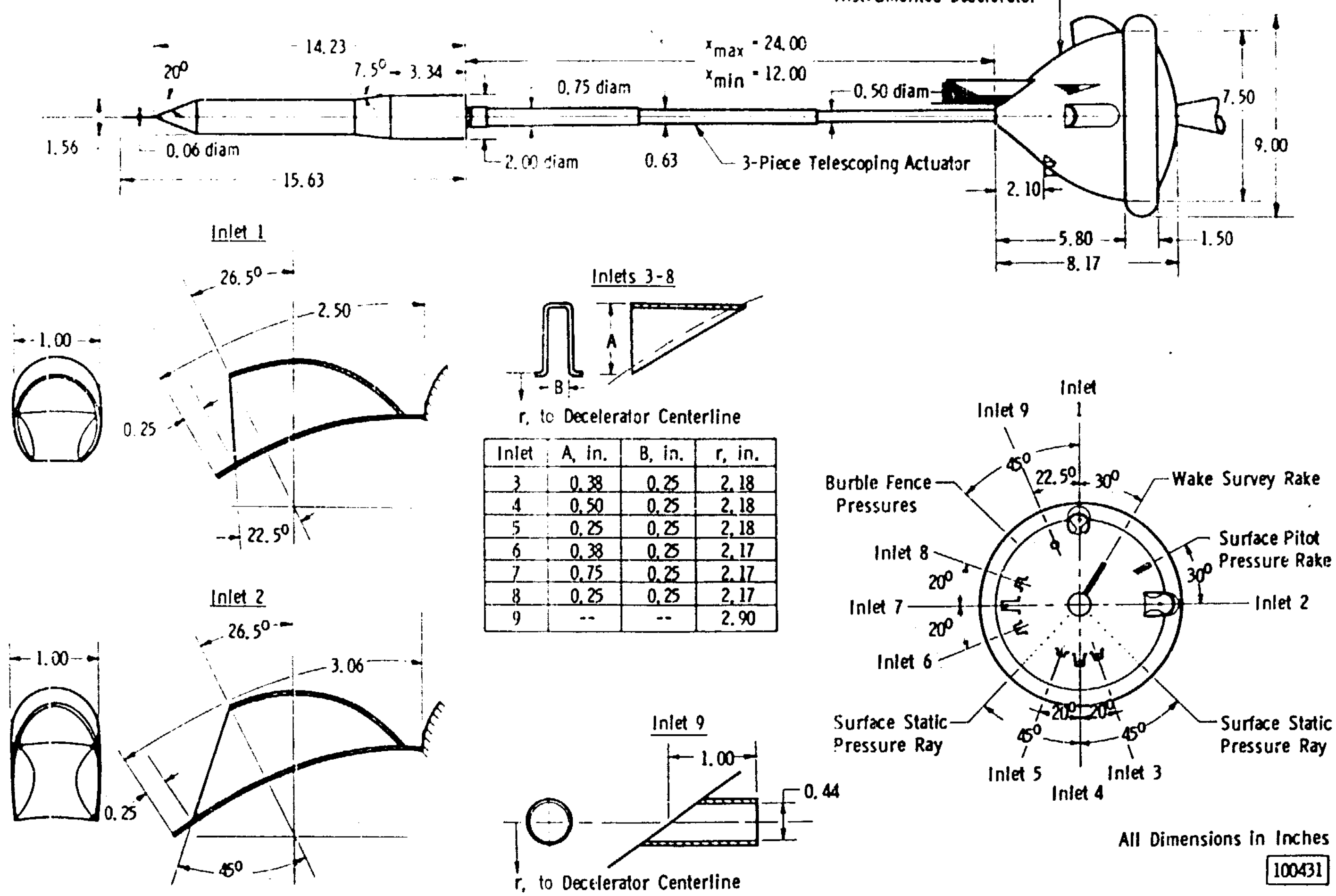

Inlet	A, in.	B, in.	r, in.
3	0.38	0.25	2.18
4	0.50	0.25	2.18
5	0.25	0.25	2.18
6	0.38	0.25	2.17
7	0.75	0.25	2.17
8	0.25	0.25	2.17
9	--	--	2.90

a. **General Layout and Inlets**

Fig. 2 Model Geometry

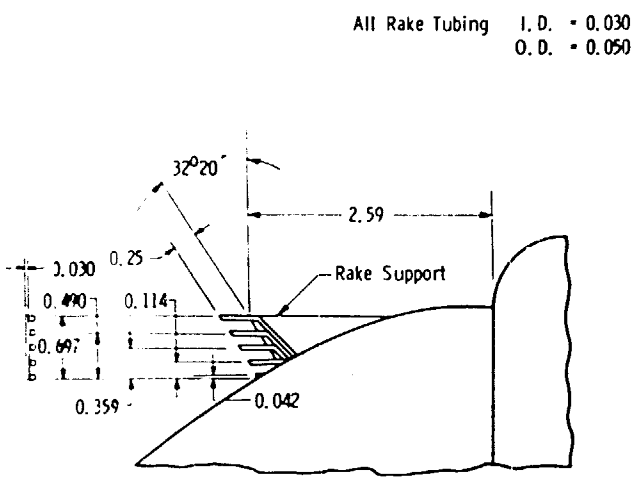

Surface Pitot Pressure Rake

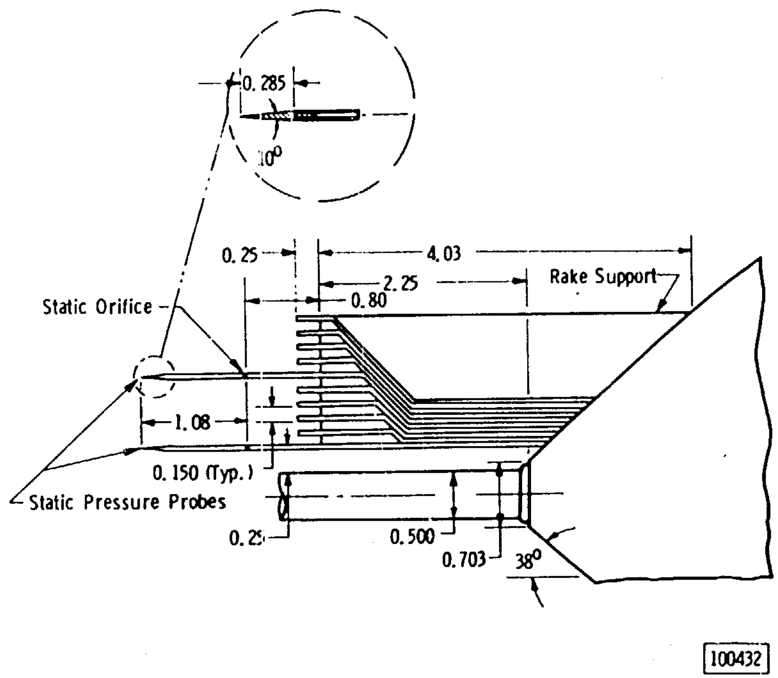

Wake Survey Rake

b. Model Rakes

Fig. 2 Concluded

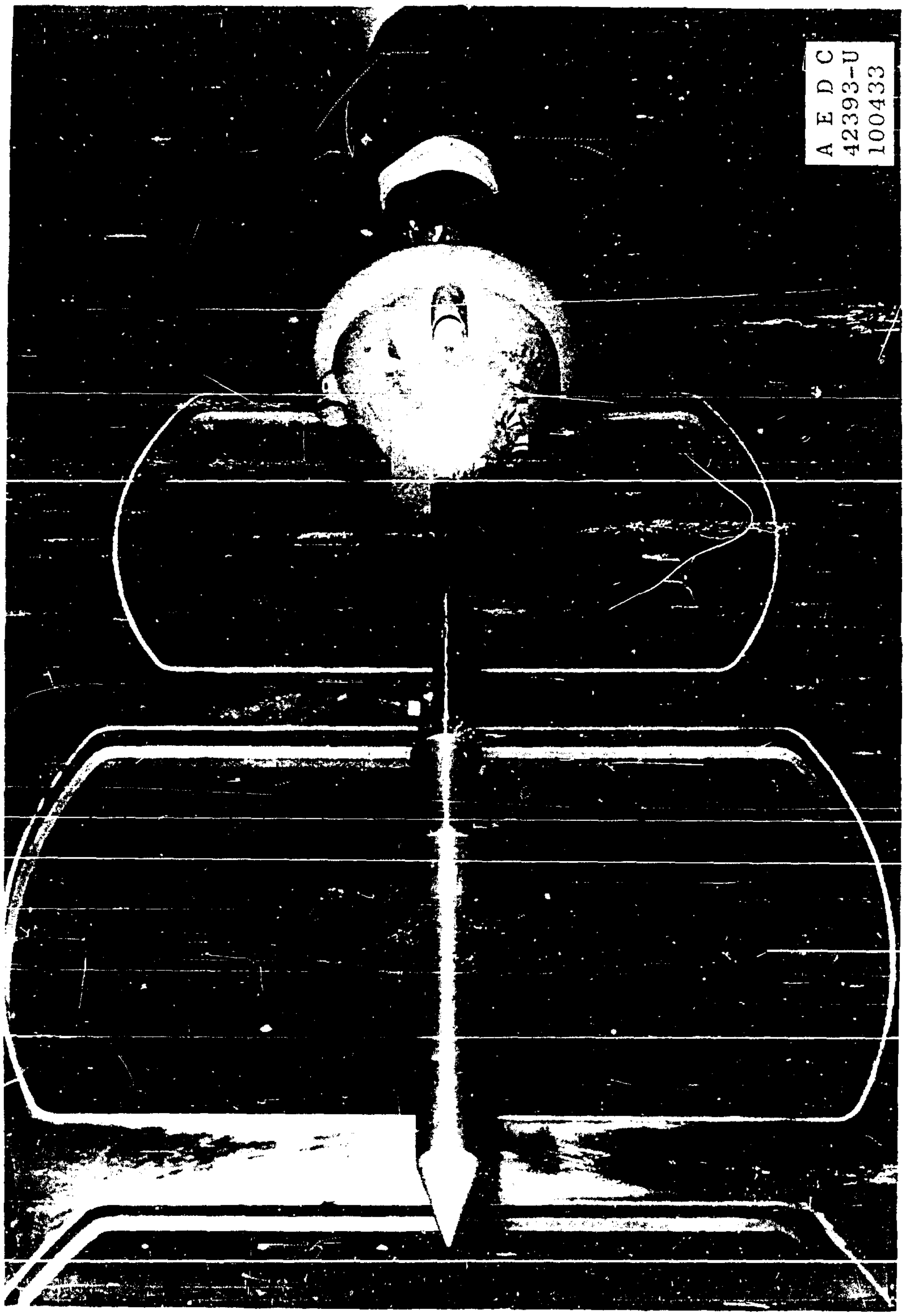

Fig. 3 Installation Photograph

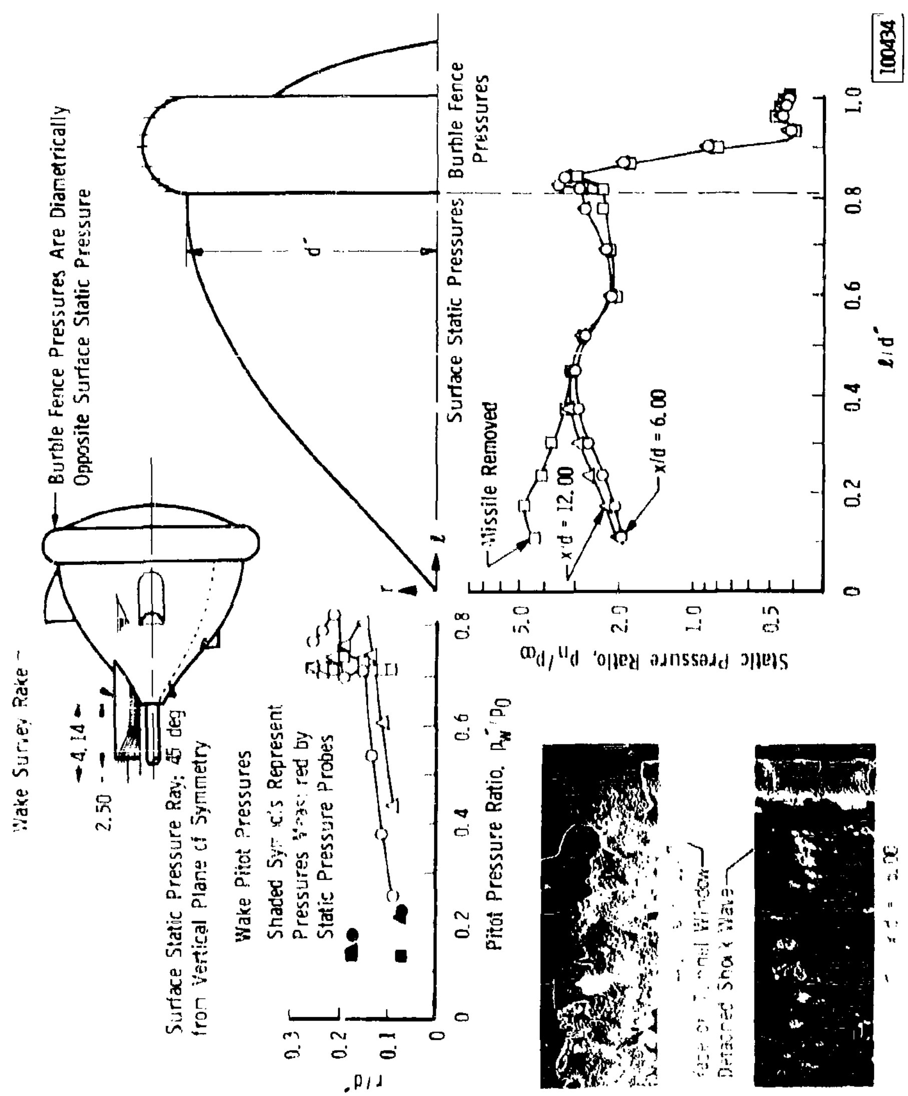

Fig. 4 Decelerator Pressure Distribution, Mach 2

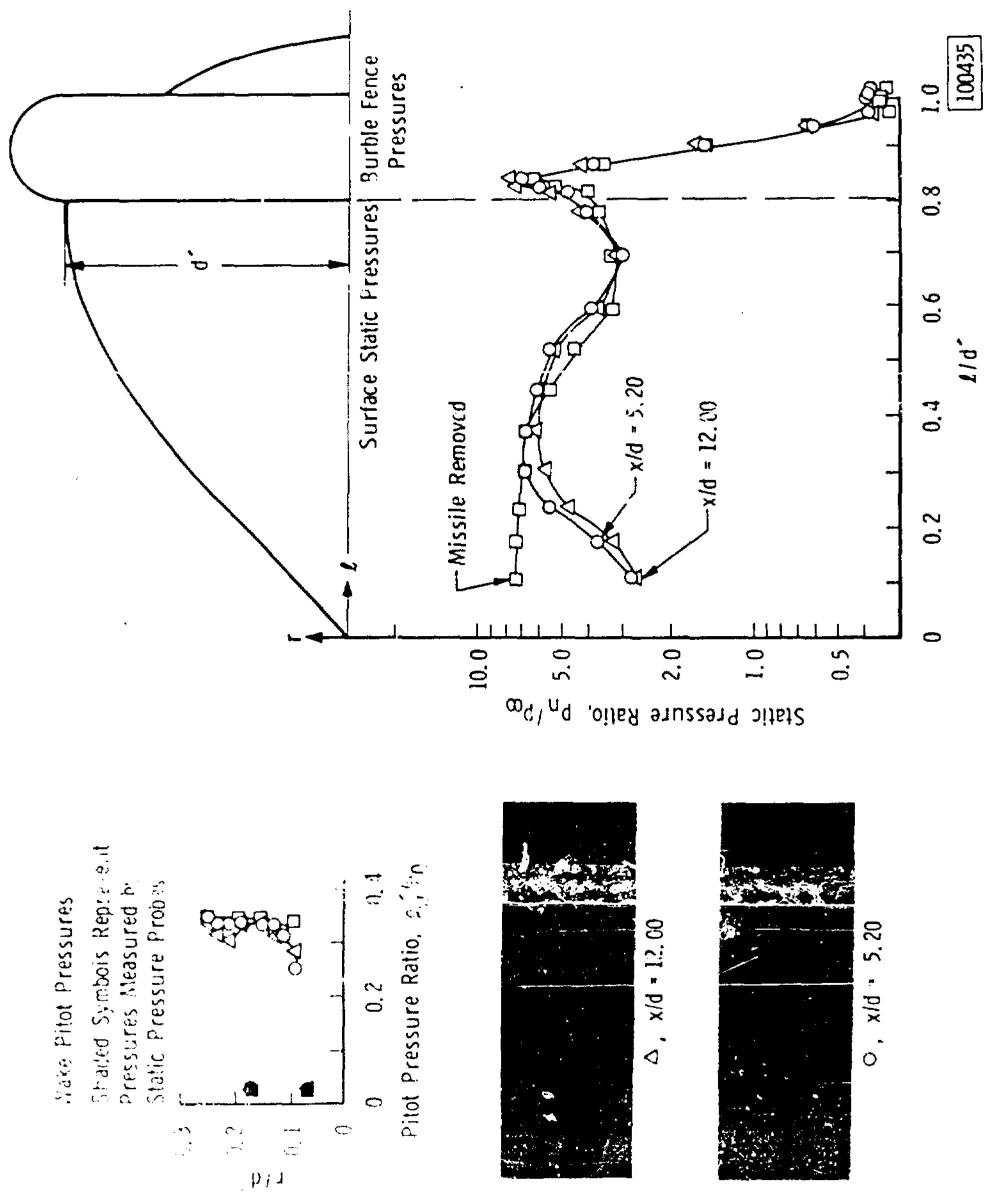

Fig. 5 Decelerator Pressure Distribution, Mach 3

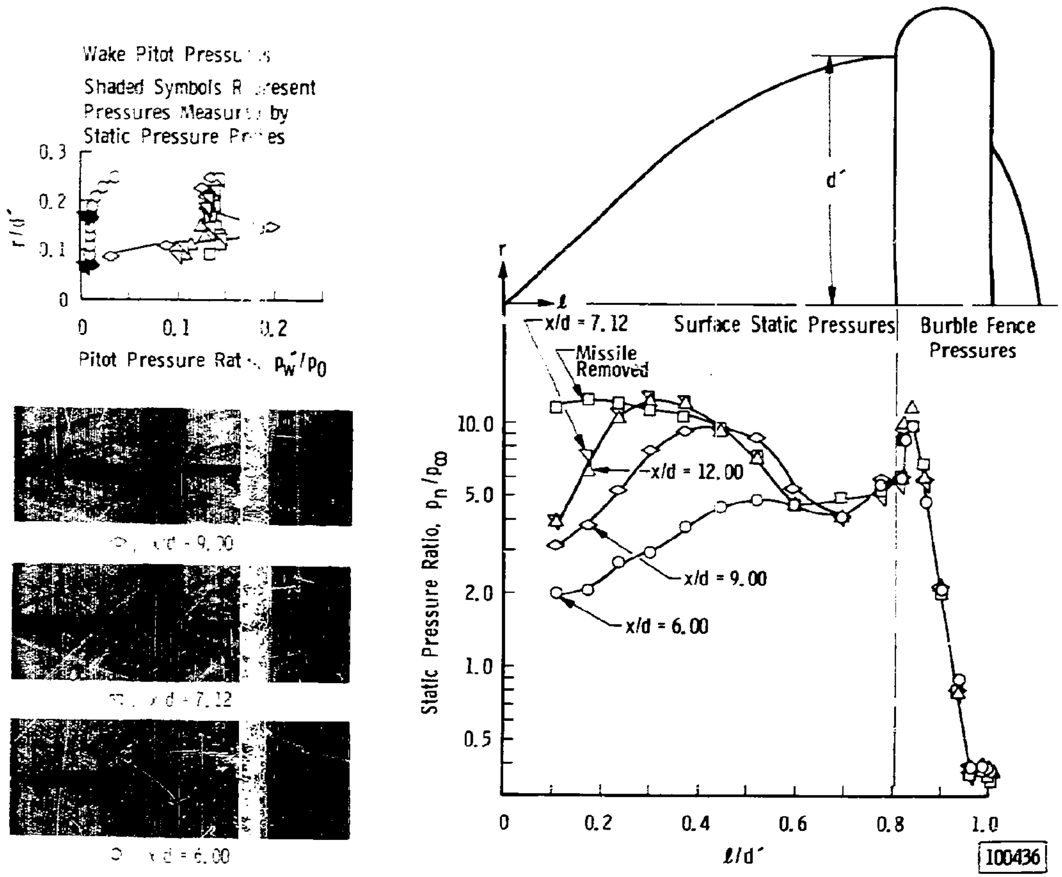

Fig. 6 Decelerator Pressure Distribution, Mach 4

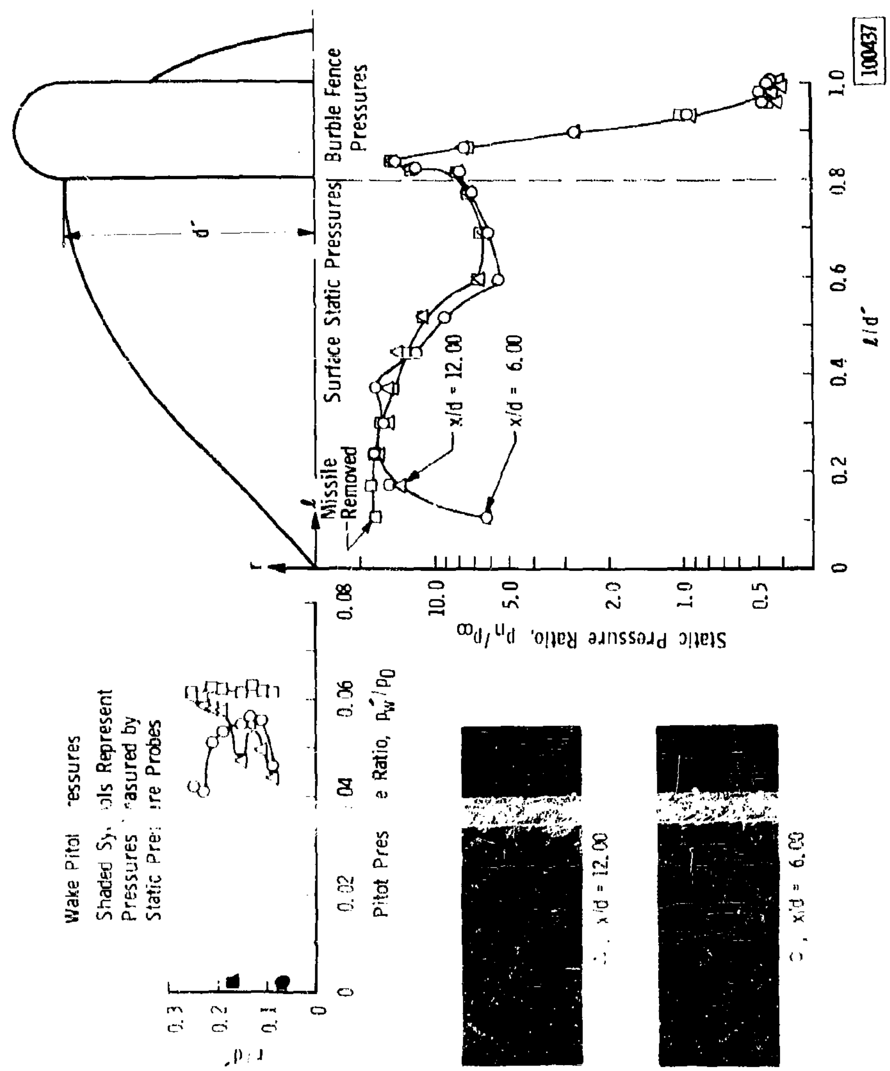

Fig. 7 Decelerator Pressure Distribution, Mach 5

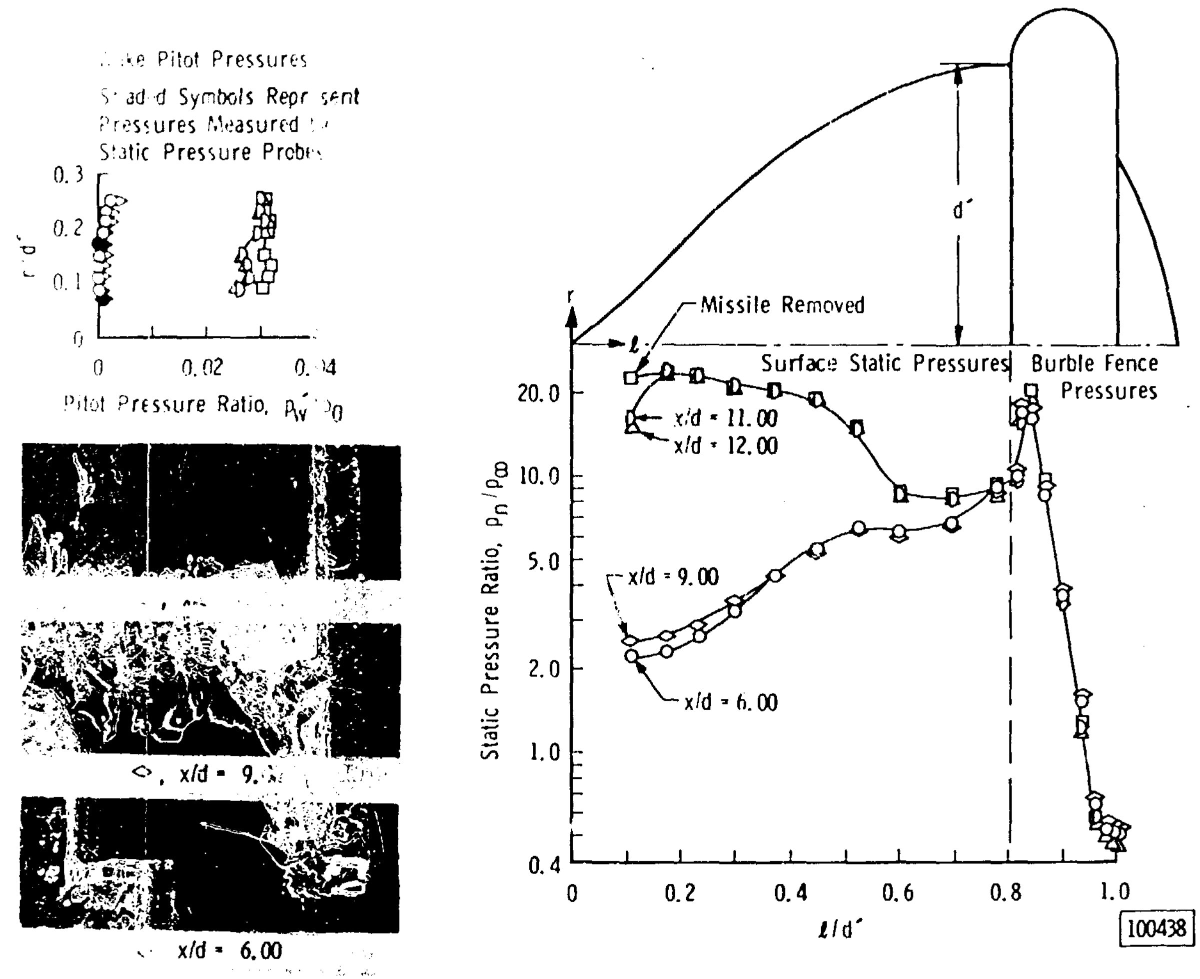

Fig. 8 Decelerator Pressure Distribution, Mach 6